Phosphorescent Platinum(II) and Palladium(II) Complexes with Azatetrabenzoporphyrins—New Red Laser Diode-Compatible Indicators for Optical Oxygen Sensing

Sergey M. Borisov,* Gunter Zenkl, and Ingo Klimant

Institute of Analytical Chemistry and Food Chemistry, Graz University of Technology, Stremayrgasse 16, 8010 Graz, Austria

ABSTRACT A new class of oxygen indicators is described. Platinum(II) and palladium(II) complexes of azatetrabenzoporphyrins occupy an intermediate position between tetrabenzoporphyrins and phthalocyanines and combine features of both. The new dyes are excitable in the red part of the spectrum and possess strong room-temperature NIR phosphorescence. Other features include excellent spectral compatibility with the red laser diodes and 632.8 nm line of He—Ne laser, excellent photostability, and significantly shorter decay times than for the respective *meso*-tetraphenyltetrabenzoporphyrins. Applicability of the complexes for optical oxygen sensing is demonstrated.

KEYWORDS: porphyrin • phosphorescence • platinum • palladium • oxygen sensor • imaging

INTRODUCTION

Phosphorescent metal complexes are known to be of great practical interest and are successfully applied in many fields of science and technology. They were demonstrated to be useful in OLEDs (1—4), photovoltaics (5—7), as singlet oxygen sensitizers for photodynamic therapy (8) and photocatalysis (9, 10), as well as labels (11, 12). Phosphorescent metal complexes are indicators of choice in optical oxygen sensors (13). Oxygen indicators such as ruthenium(II) polypyridyl complexes (14—17), platinum(II) and palladium(II) porphyrins (18—20) have been extensively used for more than a decade. The iridium(III) coumarin complexes (21, 22) introduced more recently are promising for designing ultrabright optodes (23). Notably, all these indicators are excitable with UV, blue or green light, which is a limiting factor for certain applications. Excitation in the red part of the spectrum is strongly preferred for sensing and imaging of oxygen and glucose (via oxygen transduction) in highly scattering media and in tissues (24—26). Thus, indicators with excitation and emission matching the optical window of tissue ($\sim$620—950 nm) are required for these applications. Therefore, even platinum(II) and palladium(II) complexes with porphyrin-lactones (λ_{exc} = 574 and 584 nm, respectively) (27) and porphyrin-ketones (λ_{exc} = 592 and 602 nm, respectively) (28) are not suitable here (29). Phosphorescent palladium(II) and platinum(II) complexes of tetra-benzoporphyrins (3, 30—32) and tetranaphthoporphyrins (2, 32—34) show more favorable spectral properties and are excitable at 600—640 and 690—720 nm, respectively. They possess moderate to high brightnesses (defined as a product of molar absorption ε and luminescence quantum yield QY) and relatively long phosphorescence decay times of 8—400 μs, which makes these complexes particularly suitable for optical oxygen sensing especially in biological samples and in tissues (24—26, 29). Depending on the polymer used, the complexes of tetrabenzoporphyrins possess moderate to high photostability (29, 35), but those of tetranaphthoporphyrins photobleach more readily (36). On the other hand, phthalocyanines (which are closely related to tetrabenzoporphyrins) are known for their excellent chemical, thermal, and photostability (37). They possess very narrow absorption bands in the red part of the spectrum. However, phosphorescence of the platinum(II) and palladium(II) phthalocyanines is poor (QY < 1 %) (38), which makes them hardly suitable for optical sensing and imaging of oxygen. In this contribution, we will demonstrate that platinum(II) and palladium(II) complexes of azatetrabenzoporphyrins occupy intermediate position between tetrabenzoporphyrins and phthalocyanines and combine the advantages of both, which makes them particularly suitable for application in optical oxygen-sensing materials.

EXPERIMENTAL SECTION

Materials. Phenylacetic acid, zinc oxide, methansulfonic acid, benzonitrile, aluminum oxide (activated, neutral Brockmann I), 2,9,16,23-tetra-tert-butylphthalocyanine were bought from Aldrich (www.sigmaaldrich.com); 1,3-diiminoisoindoline from TCI Europe (www.tcieurope.eu); platinum(II) chloride, palladium(II)
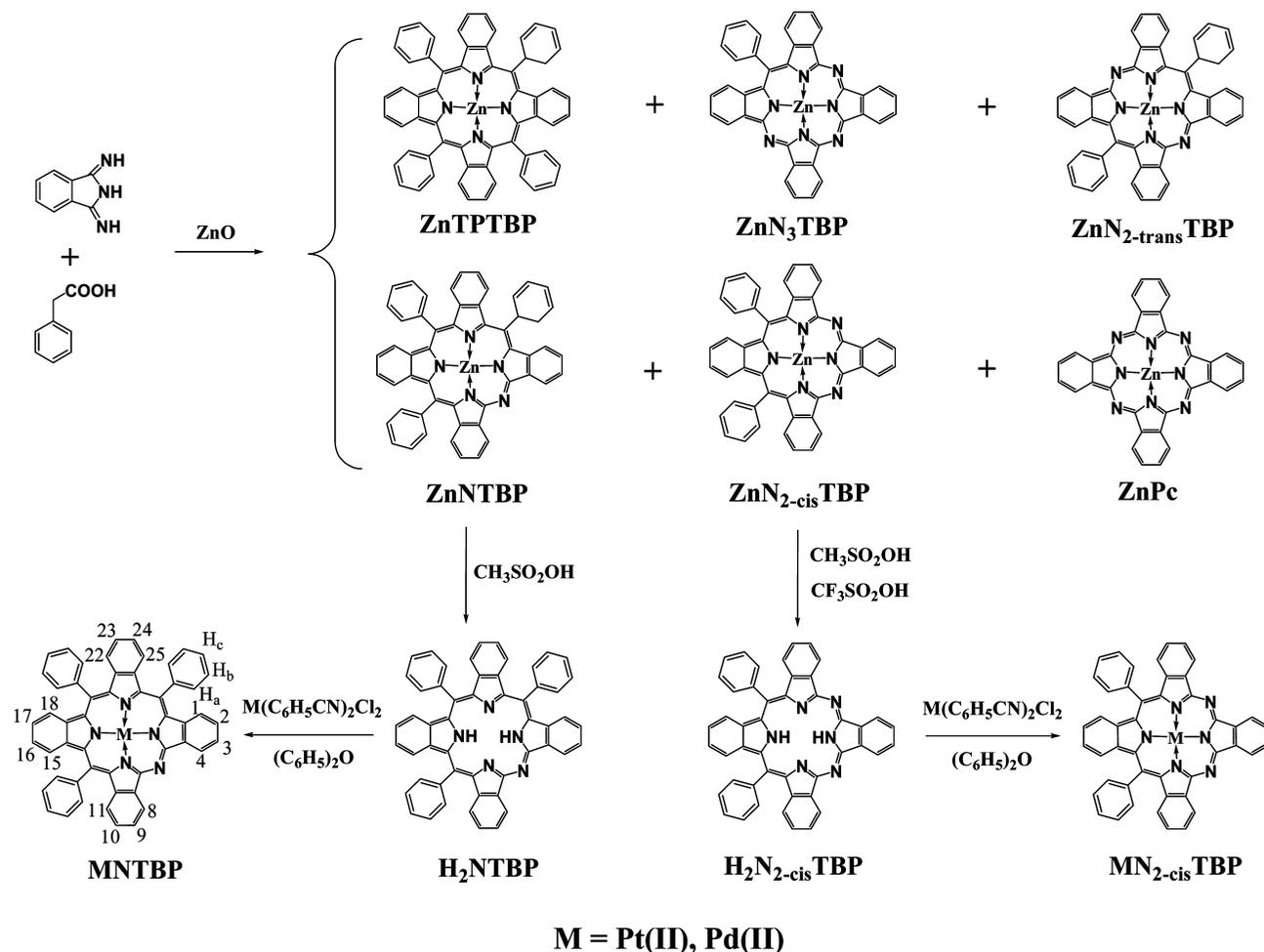
FIGURE 1. Synthesis of platinum(II) and palladium(II) azatetrabenzoporphyrin complexes.

chloride and silicagel from ABCR (www.abcr.de); polystyrene (MW 250 000) from Fisher Scientific (www.fishersci.com); poly(ethylene glycol terephthalate) support (Mylar) from Goodfellow (www.goodfellow.com); platinum(II) octaethylporphyrin (= PtOEP) from Frontier Scientific (www.frontiersci.com); Eudragit RL 100 (~10 % of quaternary ammonium groups, MW ~150 000) from Degussa (www.degussa.de). All other solvents were from Roth (www.carl-roth.de). Nitrogen, synthetic air, and test gas (1 % oxygen in nitrogen) (all of 99.999 % purity) were obtained from Air Liquide (www.airliquide.at).

Pt(C₆H₅CN)₂Cl₂ and Pd(C₆H₅CN)₂Cl₂ were obtained by dissolving platinum(II) and palladium(II) chlorides, respectively, in hot benzonitrile, and subsequent precipitation of the resulted complexes with hexane.

Preparation of the platinum(II) and palladium complexes with *meso*-tetraphenyltetrabenzoporphyrin (PtTPTBP and PdTPTBP) is described elsewhere (3, 39).

Synthesis of Zinc Azatetrabenzoporphyrins. The synthesis of the zinc complexes of azatetrabenzoporphyrins was performed using a modified literature procedure (40), Figure 1. In short, 1,3-diiminoisoindoline (14.51 g, 100 mmol), phenylacetic acid (13.62 g, 100 mmol), and zinc oxide (4.07 g, 50 mmol) were thoroughly mixed and heated to 260 °C under nitrogen. The melt was stirred for 40 min at this temperature. The resulting black tarry substrate was dissolved in acetone and the blue crystals of zinc phthalocyanine were separated. Zinc azatetrabenzoporphyrins were precipitated from the acetone solution with water. Purification was performed on an aluminum oxide column by subsequently eluting with hexane, toluene, and dichloromethane to remove impurities. Zinc 6-aza-

13,20,27-triphenyltetrabenzoporphyrin and zinc 6,13-diaza-20,27-diphenyltetrabenzoporphyrin were eluted with 2 and 7% v/v tetrahydrofuran in dichloromethane, respectively. The zinc azatetrabenzoporphyrin complexes were further purified on silica gel using dichloromethane as an eluent.

Zinc 6-Aza-13,20,27-triphenyltetrabenzoporphyrin (Zn-NTBP). Yield: 80 mg (0.4%). UV−vis (CHCl₃), λ/nm (relative intensity): 439 (1.00), 607 (0.11), 636 (0.25), 657 (0.58). MS (MALDI): m/z [M]⁺ calcd 801.1871, found 801.1891. ¹H NMR (300 MHz, DMSO-d6), ppm: 9.59 (d; 2H; H 4,8), 8.24−7.94 (m; 15H; Hₐ, H_b, H_c), 7.72−7.57 (m; 4H; H 2,3,9,10), 7.36−7.27 (m; 4H; H 1,11,15,25), 7.14−7.06 (d; 2H; H 16,24), 6.96−6.87 (m; 4H; H 17,18,22,23).

Zinc 6,13-Diaza-20,27-diphenyltetrabenzoporphyrin (ZnN₂-cisTBP). Yield: 24 mg (0.14%). UV−vis (CHCl₃), λ/nm (relative intensity): 398 (0.44), 430 (0.86), 590 (0.15), 650 (1.00), 678 (0.14).

MS (MALDI): m/z [M]⁺ calcd 726.1511, found 726.1520. ¹H NMR (300 MHz, DMSO-d6), ppm: 9.57 (d; 2H; H 8,11), 9.48 (dd; 2H; H 9,10), 8.30 (dd; 2H; H 3,16), 8.20−7.95 (m; 12H; Hₐ, H_b, H_c, H 4,15), 7.72−7.61 (m; 2H; H 1,18), 7.32 (dd; 2H; H 2,17), 7.00 (dd; 2H; H 23,24), 6.81 (d; 2H; H 22,25).

Preparation of the Free-Base Azatetrabenzoporphyrins. Seventy-five milligrams of ZnNTBP was dissolved in 15 mL of methansulfonic acid and the color changed from green to deep red, indicating the formation of the protonated form of the free-base porphyrin. The solution was poured into excess of water, the precipitated porphyrin was collected, washed several times with water and dried. In case of ZnN₂-cisTBP (20 mg) a mixture of methansulfonic acid and trifluoromethansulfonic acid (2:1,

v/v) was used for the demetalation and the operation was repeated twice. The free-base porphyrins were dissolved in dichloromethane and precipitated with methanol.

6-Aza-13,20,27-triphenyltetrabenzoporphyrin (H₂NTBP). Yield: 55 mg, 80 %. UV−vis (CHCl₃), λ/nm (relative intensity): 427 (1.00), 448 (0.95), 633 (0.44), 676 (0.49). MS (MALDI): m/z [M]⁺ calcd 739.2736, found 739.2710. ¹H NMR (300 MHz, DMSO-d6), ppm: 9.44 (d; 2H; H 4,8), 8.22 (d; 6H; H_a), 8.13−7.90 (m; 11H; H_b, H_c, H 3,9), 7.72 (t; 2H; H 2,10), 7.40−7.28 (m; 4H; H 1,11,15,25), 7.14−7.05 (m; 2H; H 16,24), 7.05−6.96 (d; 2H; H 18,22), 6.96−6.85 (m; 2H; H 17,23).

6,13-Diaza-20,27-diphenyltetrabenzoporphyrin (H₂N₂-cis-TBP). Yield: 13 mg, 70 %. UV−vis (CHCl₃), λ/nm (relative intensity): 389 (0.99), 421 (1.00), 631 (0.87), 675 (1.00). ¹H NMR (300 MHz, DMSO-d6), ppm: 9.50−9.32 (m; 4H; H 8,9,10,11), 8.33 (dd; 2H; H 3,16), 8.23−7.90 (m; 12H; H_a, H_b, H_c, H 4,15), 7.73−7.67 (m; 2H; H 1,18), 7.42 (dd; 2H; H 2,17), 7.02 (dd; 2H; H 23,24), 6.77 (d; 2H; H 22,25).

Synthesis of Platinum(II) and Palladium(II) Complexes with 6-Aza-13,20,27-triphenyltetrabenzoporphyrin. The metalation of azatetrabenzoporphyrins was performed following to the method reported previously (41). H₂NTBP (15 mg, 0.02 mmol) and Pt(C₆H₅CN)₂Cl₂ (15 mg, 0.03 mmol) or Pd(C₆H₅CN)₂Cl₂ (11 mg, 0.03 mmol) were dissolved in 4 mL of diphenylether. The solution was stirred at 160 °C until the whole free-base porphyrin was converted to the complex. The progress of the reaction was monitored with UV/vis spectroscopy. The reaction was completed in 30 min in case of the palladium(II) complex and in 60 min in case of the platinum(II) porphyrin. The products were precipitated with hexane and purified on aluminum oxide. The complexes were eluted with warm (40 °C) toluene:chloroform mixtures (9:1, 3:1, 1:1, and 1:3 v/v) and then with 1 % of ethylacetate in chloroform.

Platinum(II) and palladium(II) complexes with 6,13-diaza-20,27-diphenyltetrabenzoporphyrin were prepared in a similar manner, 6 mg (0.01 mmol) of the free-base porphyrin were used.

Platinum(II) 6-Aza-13,20,27-triphenyltetrabenzoporphyrin (PtNTBP). Yield: 13.5 mg (71 %). MS (MALDI): m/z [M]⁺ calcd 931.2206, found 931.2238. ¹H NMR (300 MHz, DMSO-d6), ppm: 9.53 (d; 2H; H 4,8), 8.28−7.97 (m; 15H; H_a, H_b, H_c), 7.77−7.65 (m; 4H; H 2,3,9,10), 7.42−7.30 (m; 4H; H 1,11,15,25), 7.12−7.04 (d; 2H; H 16,24), 6.96−6.82 (m; 4H; H 17,18,22,23).

Palladium(II) 6-Aza-13,20,27-triphenyltetrabenzoporphyrin (PdNTBP). Yield: 13 mg (76 %). MS (MALDI): m/z [M]⁺ calcd 841.1621, found 841.1595. MS (MALDI): m/z [M]⁺ calcd 801.1871, found 801.1891. ¹H NMR (300 MHz, DMSO-d6), ppm: 9.51 (d; 2H; H 4,8), 8.23−7.91 (m; 15H; H_a, H_b, H_c), 7.75−7.63 (m; 4H; H 2,3,9,10), 7.39−7.29 (m; 4H; H 1,11,15,25), 7.13−7.05 (d; 2H; H 16,24), 6.98−6.85 (m; 4H; H 17,18,22,23).

Platinum(II) 6,13-Diaza-20,27-diphenyltetrabenzoporphyrin (PtN₂-cisTBP). Yield: 3 mg (39 %). MS (MALDI): m/z [M]⁺ calcd 856.1846, found 856.1880.

Palladium(II) 6,13-Diaza-20,27-diphenyltetrabenzoporphyrin (PdN₂-cisTBP). Yield: 4 mg (58 %). MS (MALDI): m/z [M]⁺ calcd 766.1260, found 766.1226.

Preparation of the Sensor Films. The "cocktails" for coating were prepared by dissolving 1 mg of an indicator and 200 mg of polystyrene in 1800 mg of chloroform. The cocktails were knife-coated on Mylar support to give, after solvent evaporation, phosphorescent sensor films of ∼2.5 μm thick.

Preparation of the Dye-Loaded Nanoparticles. Two-hundred milliliters of distilled water was added under vigorous stirring to the solution containing 100 mg of RL-100 and 0.4 mg of PtNTBP in 50 mL of THF. All THF and partly water were removed under reduced pressure.

Measurements. Mass spectrometry was performed on a Micromass TofSpec 2E time-of-flight mass spectrometer as described in detail previously (39). Absorption spectra were

recorded on a Cary 50 UV/vis spectrophotometer (www.lzs-concept.com). Emission spectra were acquired on a QE65000 spectrometer from Ocean Optics (www.oceanoptics.com) optimized for the spectral range of 300−1050 nm. The emission spectra were corrected for the sensitivity of the photodetector which was calibrated using a halogen lamp. Luminescence decay times and quantum yields were measured using a lock-in-amplifier from PreSens (www.presens.de) equipped with a silicone photodiode. Oxygen was removed by bubbling nitrogen through the solution for 15 min. The relative quantum yields for the azatetrabenzoporphyrins were determined as an average of three values: obtained under excitation with a 635 nm laser diode from Roithner (www.roithner-laser.com) and a 628 nm LED from Roithner using PdTPTBP (QY = 0.21) (39) as a standard and under excitation with a 405 nm LED from Roithner using PtOEP as a standard (QY = 0.415) (42). The light of the violet LED was filtered through a BG-12 filter from Schott (www.schott.com), a NIR-blocking Calflex X filter (www.linos.com) was used for the red LED, and no filters for the laser-diode. In all cases, a long-pass RG-9 (Schott) filter was used for the emission. For the decay time, determination modulation frequencies of 5493 and 916 Hz were used for the Pd(II) and Pt(II) complexes, respectively. Temperature was kept constant at 25 °C using a cryostat ThermoHaake DC50.

Oxygen quenching in toluene and polystyrene was studied using a lock-in-amplifier from PreSens. A 628 nm LED was used for the excitation together with the Calflex X filter, and an RG-9 filter for the emission. Mixtures of oxygen and nitrogen obtained using a gas mixing device (MKS, www.mksinst.com) were bubbled through a cuvette with toluene solution of an indicator or were guided through a 4 mL glass vial containing a sensor foil.

Photobleaching experiments were performed with solutions of the dyes in dimethylformamide in a 1 mm cuvette. A 3 W 631 nm LED was used for excitation. The reaction progress was controlled via absorption spectrometry. The cuvette was shaken every 90 s to provide sufficient oxygen supply.

RESULTS AND DISCUSSION

Synthesis. The complexes of Pt(II) and Pd(II) with azatetrabenzoporphyrins can be prepared in three steps (Figure 1). These include template condensation of 1,3-diiminoisoindoline with phenylacetic acid in presence of zinc oxide (following the procedure reported by Galanin et al.) (40), demetalation of the resulting zinc complexes with azatetrabenzoporphyrins and, finally, platination or palladation of the metal-free porphyrins. As expected, a variety of zinc complexes are produced in a single step via the template condensation, namely zinc phthalocyanine, zinc meso-tetraphenyltetrabenzoporphyrin and zinc azatetrabenzoporphyrins (Figure 1). Zinc phthalocyanine is virtually insoluble in organic solvents and can be removed easily. Zinc azatetrabenzoporphyrins as well as zinc meso-tetraphenyltetrabenzoporphyrin are separated by column chromatography on aluminum oxide. Zinc 6-aza-13,20,27-triphenyltetrabenzoporphyrin (ZnNTBP) can be isolated in 0.4 % yield, which is acceptable considering the low cost of the reagents and simplicity of the synthesis. The yield is significantly less than 11 % reported by Galanin et al. (40), but we were not able to increase it by varying the ratio of the reagents and reaction temperature. The rather low yields of azatetrabenzoporphyrins are explained by very rapid formation of virtually useless zinc phthalocyanine (typically 10−20 % overall yield). Microwave-assisted synthesis re-
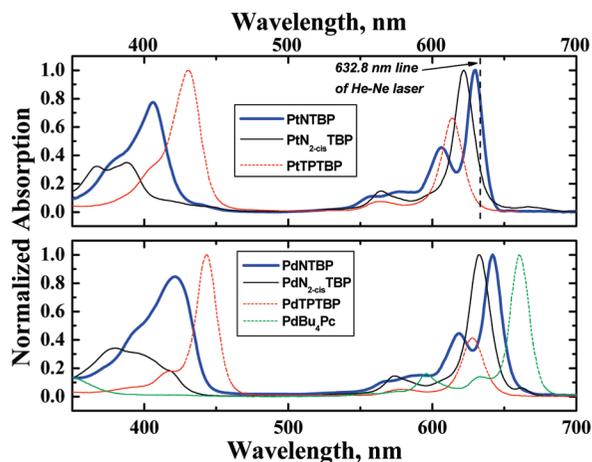
FIGURE 2. Absorption spectra of the Pt(II) and Pd(II) complexes with azatetrabenzoporphyrins NTBP and N$_{2\text{-cis}}$TBP, absorption of Pd(II) 2,9,16,23-tetra-*tert*-butylphthalocyanine (PdBu$_4$*Pc*) is also shown for comparison.

ported for phthalocyanines (43) may represent a promising possibility to improve the yields of azatetrabenzoporphyrins since 1,3-diiminoisoindoline is slowly generated in situ and may condense with phenylacetic acid rather than form phthalocyanine. In principle, it may be possible to obtain the complexes of 6-aza-13,20,27-triphenyltetrabenzoporphyrin by cyclization of a linear tetrapyrrole (analogously to the synthesis of monoazaporphyrins) (44) with subsequent aromatization of the molecule. However, 1-bromo-3-formyl-4,5,6,7-tetrahydroisoindole, a precursor for the preparation of tetrapyrrole, would be available only in a multistep synthesis. Therefore, we believe that much simpler template condensation is the most convenient route to azatetrabenzoporphyrins. It is also important that apart from ZnNTBP, other azaporphyrins can be isolated. For example, it was possible to isolate 6,13-diaza-20,27-diphenyltetrabenzoporphyrin (ZnN$_{2\text{-cis}}$TBP) in low yield, which was further used for preparation of the respective Pt(II) and Pd(II) complexes. Isolation of the zinc triazatetrabenzoporphyrin is possible, but its demetalation to the free base is extremely difficult because of increased stability of the zinc complex. In fact, it is well-known that the acidity of the N−H protons greatly increases with azo-substitution (45).

Once obtained, the zinc complexes with ZnNTBP and ZnN$_{2\text{-cis}}$TBP are demetalated with strong acids to give the respective free base porphyrins H$_2$NTBP and H$_2$N$_{2\text{-cis}}$TBP (Figure 1). The platination and palladation of the free bases is performed in good yields following to the method reported previously (41) using Pt(II) and Pd(II) bis(benzonitrile) dichlorides, respectively.

Photophysical Properties. *Absorption.* Figure 2 shows the absorption spectra of Pt(II) and Pd(II) complexes with azatetrabenzoporphyrins. They are compared to the respective complexes with *meso*-tetraphenyltetrabenzoporphyrin (TPTBP), which proved to be excellent oxygen indicators (29). In good agreement with the theoretical predictions (four orbital model of Gouterman) (46) azasubstitution results in the hypsochromic shift of the Soret band associated with the a$_{2u}$ → e$_g$ transition accompanied by the decrease

Table 1. Photophysical Properties of the Pt(Ii) and Pd(Ii) Complexes with Azatetrabenzoporphyrins

dye	λ_{max}^{abs} ($\varepsilon \times 10^{-3}$) (nm (M^{-1} cm^{-1}))	λ_{max}^{em} (nm)	Q.Y.	τ (μs)	E_T (cm^{-1})
PtTPTBP	430 (205); 564 (16); 614 (136)	770	0.51	47	13 160
PtNTBP	406 (106); 606 (61); 630 (137)	844	0.22	40	11 850
PtN$_{2\text{-cis}}$TBP	367 (47); 388 (51); 564 (21); 621 (147)	841	0.17	20	11 890
PdTPTBP	443 (416); 578 (21); 628 (173)	800	0.21	286	12 630
PdNTBP	421 (106); 619 (58); 642 (133)	875	0.08	213	11 430
PdN$_{2\text{-cis}}$TBP	380 (33); 574 (14); 631 (98)	873	0.05	101	11 460

of the molar absorption coefficient (Table 1). Azasubstitution also decreases the energy of the LUMO e$_g$ orbitals so that the Q-bands (a$_{1u}$ → e$_g$ transitions) for the complexes of NTBP and N$_{2\text{-cis}}$TBP shift bathochromically compared to TPTBP. The Q-bands of the respective phthalocyanine complexes shift further to the red (Figure 2). Interestingly, the Q bands of PtNTBP and PdNTBP are ∼10 nm red-shifted compared to PtN$_{2\text{-cis}}$TBP and PdN$_{2\text{-cis}}$TBP. This effect is attributed to the decrease in π-conjugation of the *meso*-phenyl substituents (33) and is similar to that observed in case of *meso*-unsubstituted tetrabenzoporphyrins, which absorb at shorter wavelengths than the *meso*-phenylsubstituted analogues (47). PtNTBP, particularly, shows excellent compatibility with 632.8 nm line of the He−Ne laser and 635 nm red laser diode already in toluene solution, which is of much interest for potential applications in optical sensing and microscopy. Similarly to other porphyrins, the absorption bands of PtNTBP embedded in polystyrene are bathocromically shifted compared to their position in toluene solution. In fact, in polystyrene, the Q-band of the complex is located exactly at 633 nm. Considering the respective Pd(II) complex, the Q-band is located at 642 nm in toluene (Table 1) and at 645 nm in polystyrene. Thus, the dye can be efficiently excited with 645 and 650 nm red laser diodes.

Emission. Pt(II) and Pd(II) complexes with NTBP and N$_{2\text{-cis}}$TBP represent a new class of NIR emitting dyes that possess strong room-temperature phosphorescence in deoxygenated solution and in polymers (Figure 3). A bathochromic shift of ∼80 nm of the emission band is observed for the azotetrabenzoporphyrin complexes compared to the parent *meso*-tetraphenyltetrabenzoporphyrins. The positions of the emission bands for the NTBP and N$_{2\text{-cis}}$TBP complexes are similar. In respect to absorption and emission, the azatetrabenzoporphyrins occupy an intermediate position between *meso*-tetraphenyltetrabenzoporphyrins and phthalocyanines. In fact, the phosphorescence of phthalocyanines complexes is located at much longer wavelength (e.g., 1020 nm for Pd(II) 2,9,16,23-tetra-*tert*-butylphthalocyanine) (48). Interestingly, the emission bands of the monoaza-substituted complexes are narrower than for the *meso*-tetraphenyltetrabenzoporphyrins (fwhm 350, 685, 390, and 710 cm^{-1} for PtNTBP, PtTPTBP, PdNTBP, and PdTPTBP, respectively). However, the emission bands of the N$_{2\text{-cis}}$TBP complexes are broader than for the NTBP dyes (fwhm 540 and 570 cm^{-1}
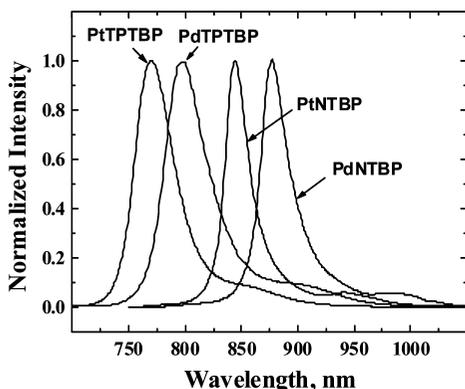
FIGURE 3. Emission spectra of Pt(II) and Pd(II) azatetrabenzoporphyrin and *meso*-tetaphenyltetrabenzoporphyrin complexes in deoxygenated toluene at RT.

for PtN$_{2\text{-cis}}$TBP, PdN$_{2\text{-cis}}$TBP, respectively). Luminescence decay times (τ) and quantum yields (Q.Y.) are summarized in Table 1. The Pt(II) and Pd(II) complexes with azatetrabenzoporphyrins are seen as weaker emitters than the respective *meso*-tetraphenyltetrabenzoporphyrins PtTPTBP and PdTPTBP. Despite this, the brightness of the indicators (BS, defined as the product of molar absorption coefficient ε and luminescence quantum yield) is adequate for practical applications. The BS of PtNTBP in the maximum of the Q-band is 25 000 which is still much higher than for many common oxygen indicators such as Ru(II) tris-4,7-diphenylphenanthroline (BS $\approx$ 10 500) (49), Pt(II) *meso*-pentafluorophenylporphyrin (BS $\approx$ 4000) (50) and Pt(II) octaethylporphyrin ketone (BS $\approx$ 7000) (28). Evidently, the substitution of *meso*-phenyl rings by nitrogen atoms results in a decrease of the luminescence quantum yields. In fact, in case of PdBu$_4$*Pc* the Q.Y. was estimated to be only 0.02. That is in a good agreement with the literature data (38, 51) demonstrating that the Pt(II) phthalocyanine complex is a rather poor emitter. Azasubstitution is also found to shorten of the luminescence decay time (Table 1). The reduction of the luminescence quantum yields and shortening of the luminescence decay times can be explained by increased probability of the nonradiative deactivation of the triplet excited state. In fact, the following trend is observed for the energies of the triplet excited state: TPTBP > NTBP $\cong$ N$_{2\text{-cis}}$TBP > Bu$_4$*Pc* so that nonradiative processes become more likely. A similar trend was observed in case of Pt(II) and Pd(II) complexes with *meso*-tetraphenyltetranaphthoporphyrin (TPTNP) that emit at significantly longer wavelengths than the respective complexes with *meso*-tetraphenyltetrabenzoporphyrin. In fact, the luminescence quantum yields and the decay times were reported to be 0.51 and 47 μs for PtTPTBP (λ_{max}^{em} = 770 nm) (39), 0.22 and 8.5 μs for PtTPTNP (λ_{max}^{em} = 883 nm) (2), 0.21 and 286 μs for PdTPTBP (λ_{max}^{em} = 800 nm) (39), 0.065 and 65 μs for PdTPTNP (λ_{max}^{em} = 937 nm) (33). It can be concluded here that the complexes of NTBP represent excellent candidates for practical applications, but the properties of the N$_{2\text{-cis}}$TBP complexes are much less favorable because of lower luminescence brightness.

Photostability. Figure 4 shows the absorption spectra of the PdNTBP in air-saturated dimethylformamide irradi-

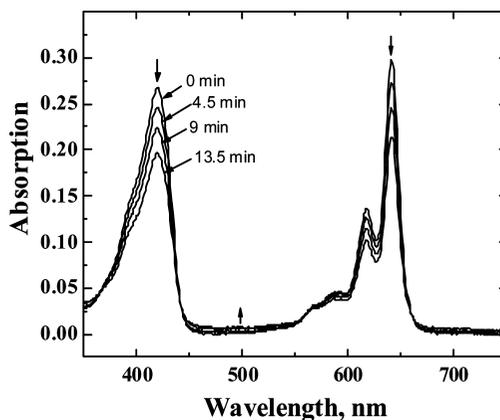**FIGURE 4.** Spectral changes upon irradiation of air-saturated solution of PdNTBP in dimethylformamide with the light of a 631 nm 3W LED.
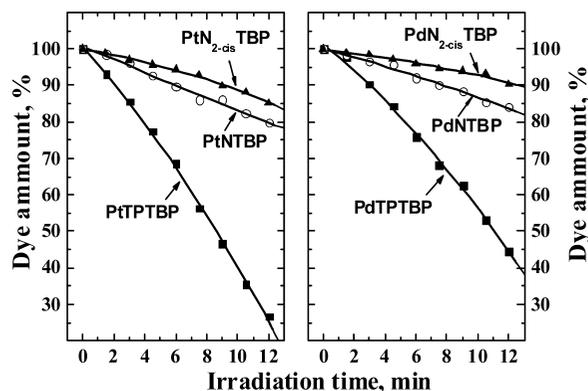

FIGURE 5. Photodegradation of the Pt(II) and Pd(II) complexes in air-saturated dimethylformamide solution. Irradiation is performed with a 631 nm 3W LED.

ated with the red light of a 631 nm LED. The dye is irreversibly destroyed and no colored/luminescent products are formed. Figure 5 shows the photodegradation of Pt(II) and Pd(II) complexes. The respective Pt(II) and Pd(II) complexes with *meso*-tetraphenyltetrabenzoporpyrin were taken for comparison. The photostability of these dyes was shown to be similar or higher (depending on the matrix used) than that of Pt(II) octaethylporphyrin, a commonly used oxygen indicator, but was significantly lower than that of very photostable Pt(II) 5,10,15,20-*meso*-pentafluorophenylporphyrin (29, 35). As can be seen, the complexes with NTBP and N$_{2\text{-cis}}$TBP prove to be much more photostable than the respective *meso*-tetraphenyltetrabenzoporpyrins. PtN$_{2\text{-cis}}$TBP and PdN$_{2\text{-cis}}$TBP are more photostable than the monoazatetrabenzoporphyrin complexes. It can also be concluded that the photostability of the Pd(II) complexes is only slightly better the photostability of the respective Pt(II) dyes. It should also be mentioned that all the dyes show much slower (and therefore not easily measurable) photobleaching in some other solvents such as, e.g., toluene. The complexes also show excellent photostability in such a common polymer matrix as polystyrene. It is evident that the new indicators are particularly suitable for interrogation using high light intensities, which are typical for microsensors and microscopy applications including excitation with lasers.
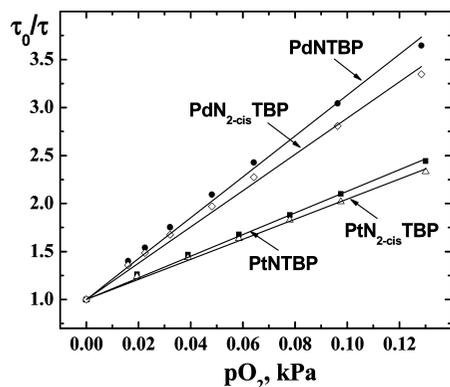
FIGURE 6. Stern−Volmer plots for oxygen quenching in solutions of the azatetrabenzoporphyrins in toluene at 25 °C.
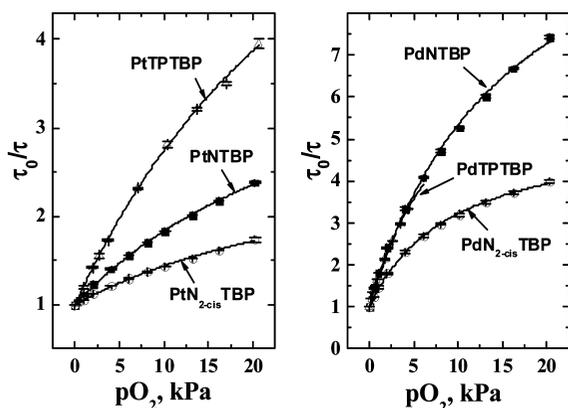

FIGURE 7. Stern−Volmer plots for oxygen quenching in polystyrene at 25 °C. The lines represent a fit according to eq 1.

Quenching by Molecular Oxygen in Solutions. In solution the phosphorescence of azatetrabenzoporphyrins is efficiently quenched by molecular oxygen (Figure 6). As expected from the luminescence decay times, the emission of the Pd(II) complexes is quenched more efficiently than for the respective Pt(II) dyes. Interestingly, the Stern−Volmer constants for complexes of NTBP and $N_{2\text{-}cis}$TBP are similar (0.0113 Pa^{-1} for PtNTBP and 0.0105 Pa^{-1} for PtN$_{2\text{-}cis}$TBP; 0.0213 Pa^{-1} for PdNTBP and 0.0189 Pa^{-1} for PdN$_{2\text{-}cis}$TBP) despite significantly longer decay times of the NTBP complexes (Table 1). Thus, the quenching constants $k_q = K_{SV}/\tau_0$ are significantly higher for the $N_{2\text{-}cis}$TBP complexes than for NTBP complexes and both exceed the k_q values obtained for *meso*-tetraphenyltetrabenzoporphyrins (k_q = 283, 523, 102, 99, 187, and 60 Pa^{-1} s^{-1} for PtNTBP, PtN$_{2\text{-}cis}$TBP, PtTPTBP (39), PdNTBP, PdN$_{2\text{-}cis}$TBP and PdTPTBP (39), respectively) which may be due to sterical reasons. Interestingly, in toluene, the quenching constants k_q are higher for the Pt(II) azatetrabenzoporphyrins than for the respective Pd(II) complexes.

Optical Oxygen Sensors. Polystyrene and its co-polymers are often polymers of choice for designing optical oxygen sensors. Polystyrene was also preferred in this study since the results can easily be compared to those obtained for other indicators in the same matrix. Figure 7 shows the Stern−Volmer plots for the Pt(II) and Pd(II) complexes with NTBP, N$_{2\text{-}cis}$TBP and TPTBP. The fit is performed with a modified equation from the "two-site

Table 2. Properties of the Dye-Doped Polystyrene Films Based on the Azatetrabenzoporphyrin Complexes (0.5% dye w/w)

indicator	λ_{max}, abs (nm)	λ_{max}, em (nm)	τ_0 (μs)	f	K_{SV} at 25 °C (kPa^{-1})	$\Delta\tau/K$ at 0 kPa (%)
PtTPTBP	432, 566, 615	772	55	0.87	0.165	0.06
PtNTBP	407, 609, 633	842	40	0.78	0.138	0.055
PtN$_{2\text{-}cis}$TBP	367, 573, 625	845	20	0.67	0.084	0.02
PdTPTBP	445, 581, 630	800	356	0.87	0.92	0.33
PdNTBP	422, 621, 645	877	250	0.92	0.76	0.50
PdN$_{2\text{-}cis}$TBP	378, 582, 536	874	125	0.81	0.57	0.17

model" (52) assuming localization of an indicator into two different regions

$$\frac{I}{I_0} = \frac{\tau}{\tau_0} = \frac{f}{1 + K_{SV}[O_2]} + 1 - f \qquad (1)$$

where f and K_{SV} are, respectively, the fraction of the total emission and the Stern−Volmer constant for the first site; the Stern−Volmer constant for the second site is assumed to be 0. It should be mentioned here that eq 1 has physical meaning only for the ratio of luminescence intensities and not the decay times. Nevertheless, it can be used to adequately fit average decay times (correlation coefficient >0.998) obtained in frequency domain. The fit parameters are summarized in Table 2. The increase in the K_{SV}/τ_0 values from TPTBP to N$_{2\text{-}cis}$TBP is similar to the trend observed for the dyes dissolved in toluene. Nevertheless, in polystyrene the Stern−Volmer constants correlate well with the luminescence decay times τ_0. Thus, the new Pt(II) complexes enable preparation of less sensitive sensors compared to PtTPTBP/PS material. This can be beneficial for some applications where oxygen partial pressures are higher that 21 kPa (for example in photosynthetic systems). In such a system, PtTPTBP/PS sensor becomes less reliable at high oxygen concentrations (because of the lower S/N ratio), but the sensors based on Pt(II) azatetrabenzoporphyrins still retain substantial dynamics. For the same reason, the new Pt(II) indicators can also be immobilized in the fast-responding polymers having rather high oxygen permeability (such as, for example, organically modified silica Ormosil) where PtTPTBP would be only suitable for trace oxygen sensing.

It should be mentioned that the solubility of the Pt(II) and Pd(II) azatetrabenzoporphyrins in polystyrene is not as good as in case of *meso*-tetraphenyltetrabenzoporphyrins. The former tend to aggregate if the concentration is rather high (>1 % w/w) which is confirmed by shortening of the luminescence decay time. As expected, the N$_{2\text{-}cis}$TBP complexes aggregate more readily than the complexes with NTBP. To avoid aggregation the concentration of azatetrabenzoporphyrins in the polymer should not exceed 0.5 % w/w. It is well-known that phenyl groups in the *meso*-positions of the porphyrin macrocycle increase solubility of the molecules in solvents and polymers, and *meso*-unsubstituted porphin,

tetrabenzoporphyrin as well as phthalocyanine are poorly soluble in organic solvents (51). The solubility of *meso*-unsubstituted molecules in such cases can be rendered by providing the macrocycle with bulky substituents (such as, e.g., *tert*-butyl). This strategy can also be used for azatetra-benzoporphyrins in order to increase their solubility.

Temperature Dependence of the Luminescence Decay Times. It is well-known that optical chemosensors for oxygen, carbon dioxide, ammonia and other gases show a cross-talk to temperature (53). In the case of the oxygen optodes, temperature affects both the decay time of an indicator (thermal quenching) and the gas permeability of a polymer. Some of the oxygen indicators (such as Ru(II) polypyridyl complexes) show severe thermal quenching (23) which may compromise the performance of the sensors. It was found that the Pt(II) complexes with azatetrabenzoporphyrins show virtually negligible thermal quenching at RT (Table 2). Temperature coefficients are substantially lower in case of $N_{2\text{-}cis}$TBP compared to the NTBP complexes. Analogously to the complexes with TPTBP, the thermal quenching is more pronounced for the Pd(II) complexes than for the Pt(II) dyes.

Imaging of Oxygen Tension. As was demonstrated above, the platinum(II) and palladium(II) complexes with azatetrabenzoporphyrins represent excellent candidates for application in oxygen sensors. These can be realized in such traditional sensor formats as planar sensor foils and spots, paints and fiber-optic sensors. On the other hand, water-dispersible sensing nanobeads, dendrimers, and macromolecular conjugates represent promising analytical tools that enable analyte sensing and imaging in solution (26, 54, 55). Because of their small size, the nanobeads are nicely suitable for microscopic applications. Red-light-excitable NIR emitting indicators are particularly promising for imaging in biological systems since background fluorescence and light scattering are minimized and thus virtually interference-free measurements become possible. PtNTBP, particularly, represents a promising candidate for such applications due to high luminescence brightness and excellent compatibility with 632.8 nm line of He–Ne laser used in confocal microscopes. Previously we demonstrated (56, 57) that a variety of charged and neutral nanobeads can be prepared via swelling and precipitation. It was found that the azatetrabenzoporphyrin complexes can also be successfully embedded into these polymeric beads. As an example, Figure 8 shows images of an aqueous dispersion of positively charged Eudragit RL-100 beads (poly(methyl methacrylate bearing quaternary ammonium groups) stained with PtNTBP and excited with a 635 nm laser diode. The emitted light as well as the reflected and strayed excitation light can be detected without an emission filter (Figure 8b). With a long-pass RG 9 filter in front of the camera only the NIR emission of PtNTBP is detected (Figure 8c). It is clearly enhanced if oxygen is removed (Figure 8d), demonstrating suitability of the beads for imaging of oxygen tension.

Two-photon-based oxygen imaging is another interesting application which was considered recently (58, 59). The
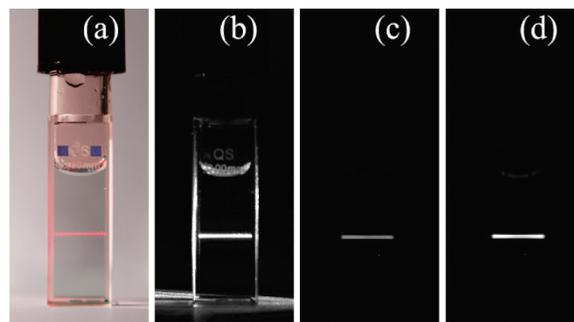

FIGURE 8. Images of an aqueous dispersion of RL-100 nanobeads (1 mg mL^{-1}) stained with PtNTBP and excited with a 635-nm laser diode: (a) a color image acquired with a Canon 5D digital camera; (b–d) images acquired with a SensiCam from PCO: (b) obtained without an emission filter; (c, d) images obtained with an RG 9 long-pass filter mounted in front of the camera, for air-saturated and oxygen-free dispersions, respectively.

azatetrabenzoporphyrins and particularly the complexes with NTBP may be much better suitable for 2-photon excitation because of their unsymmetric character, which is likely to increase the two-photon absorption cross-section (60). The suitability of the azatetrabenzoporphyrins for 2-photon oxygen imaging is currently being investigated.

In contrast to imaging applications, azatetrabenzoporphyrins should be used more carefully to design fiber-optic sensors. Here, glass optical fibers should be used, because less expensive plastic polymethylmethacrylate fibers strongly absorb at 630 nm and at wavelengths longer than 820 nm (61). This corresponds to excitation and emission maxima of azatetrabenzoporphyrins. Evidently, PtTPTBP is a much better choice here because its emission maximum corresponds to the minimum in absorption of the plastic.

Other Potential Applications. Above, we demonstrated that the new complexes are very promising for designing advanced oxygen-sensing materials. Evidently, a potential range of applications is not limited by oxygen sensors. For example, NIR-emitting OLEDs have recently drawn much attention of researches (2–4). Azatetrabenzoporphyrins (particularly PtNTBP) may provide an alternative to the OLEDs based on other NIR-emitting metal complexes. Superior photostability of azatetraphenylporphyrins compared to that of *meso*-tetraphenyltetrabenzoporphyrins and *meso*-tetraphenyltetranaphthoporphyrins (for which photobleaching is known to be rather severe) (36) is particularly advantageous here. The narrow emission peaks positioned between those of TPTBP and TPTNP may also be of interest for designing OLEDs. High photostability and good brightness of the new dyes also makes them promising for application in photovoltaic devices where suitability of PtTPTBP (5) and PtTPTNP (62) was recently demonstrated. The substitution of these dyes by much more photostable azatetrabenzoporphyrins may help to significantly extend the lifetime of the photovoltaic devices.

CONCLUSION

We showed that platinum(II) and palladium(II) complexes with azatetrabenzoporphyrins represent a new class of phosphorescent dyes that occupy intermediate position

between *meso*-tetraphenyltetrabenzoporphyrins and phthalocyanines. The azatetrabenzoporphyrin complexes possess strong room temperature phosphorescence that is efficiently quenched by molecular oxygen. The new dyes are particularly attractive as indicators for optical oxygen-sensing materials. The luminescence decay times are shorter than for the respective *meso*-tetraphenyltetrabenzoporphyrins, which enables the design of less sensitive/faster responding sensors. Compared to the complexes of *meso*-tetraphenyltetrabenzoporphyrins, the new indicators show an ~20 nm bathochromic shift of the Q-bands and thus excellent compatibility with the red 635 nm laser diode (Pt(II) complexes) and the 645 and 650 nm laser diodes (Pd(II) complexes). Among the new complexes, those with 6-aza-13,20,27-triphenyltetrabenzoporphyrin are clearly more advantageous over the complexes with 6,13-diaza-20,27-diphenyltetrabenzoporphyrin due to higher yields, better luminescence brightness and solubility. The PtNTBP in polymeric nanobeads is particularly promising for confocal imaging of oxygen tension using He−Ne laser as an excitation source. Because of their superior photostability compared to other NIR-emitting metal complexes, the new phosphorescent dyes may also find application in NIR OLEDs and photovoltaic devices.

Supporting Information Available: UV−vis spectra of the zinc complexes and the ligands, MALDI and ^{1}H NMR spectra of the ligands, zinc, platinum(II) and palladium(II) complexes (PDF). This material is available free of charge via the Internet at http://pubs.acs.org.

REFERENCES AND NOTES

(1) Williams, J. A. G.; Develay, S.; Rochester, D. L.; Murphy, L. *Coord. Chem. Rev.* **2008**, *252*, 2596−2611.

(2) Sommer, J. R.; Farley, R. T.; Graham, K. R.; Yang, Y.; Reynolds, J. R.; Xue, J.; Schanze, K. S. *ACS Appl. Mater. Interfaces* **2009**, *1*, 274−278.

(3) Borek, C.; Hanson, K.; Djurovich, P. I.; Thompson, M. E.; Aznavour, K.; Bau, R.; Sun, Y.; Forrest, S. R.; Brooks, J.; Michalski, L.; Brown, J. *Angew. Chem., Int. Ed.* **2007**, *46*, 1109−1112.

(4) Sun, Y.; Borek, C.; Hanson, K.; Djurovich, P. I.; Thompson, M. E.; Brooks, J.; Brown, J. J.; Forrest, S. R. *Appl. Phys. Lett.* **2007**, *90*, 213503/1−213503/3.

(5) Currie, M. J.; Mapel, J. K.; Heidel, T. D.; Goffri, S.; Baldo, M. A. *Science* **2008**, *321*, 226−228.

(6) Kalinowski, J.; Stampor, W.; Szmytkowski, J.; Cocchi, M.; Virgili, D.; Fattori, V.; Di Marco, P. *J. Chem. Phys.* **2005**, *122*, 154710/1−154710/16.

(7) Jung, I.; Choi, H.; Lee, J. K.; Song, K. H.; Kang, S. O.; Ko, J. *Inorg. Chim. Acta* **2007**, *360*, 3518−3524.

(8) DeRosa, M. C.; Crutchley, R. J. *Coord. Chem. Rev.* **2002**, *233−234*, 351−371.

(9) Maldotti, A.; Andreotti, L.; Molinary, A.; Borisov, S. M.; Vasil'ev, V. V. *Chem.—Eur. J.* **2001**, *7*, 3564−3571.

(10) Feng, K.; Zhang, R. Y.; Wu, L. Z.; Tu, B.; Peng, M. L.; Zhang, L. P.; Zhao, D.; Tung, C. H. *J. Am. Chem. Soc.* **2006**, *128*, 14685−14690.

(11) Papkovsky, D. B.; O'Riordan, T. C. *J. Fluoresc.* **2005**, *15*, 569−584.

(12) Lo, K. K. W.; Hui, W. K.; Chung, C. K.; Tsang, K. H. K.; Ng, D. C. M.; Zhu, N.; Cheung, K. K. *Coord. Chem. Rev.* **2005**, *249*, 1434−1450.

(13) Wolfbeis, O. S. *J. Mater. Chem.* **2005**, *15*, 2657−2669.

(14) Klimant, I.; Wolfbeis, O. S. *Anal. Chem.* **1995**, *67*, 3160−3166.

(15) Carraway, E.; Demas, J.; DeGraff, B.; Bacon, J. *Anal. Chem.* **1991**, *63*, 337−342.

(16) McEvoy, A.; McDonagh, C.; MacGraith, B. *J. Sol−Gel Sci. Technol.* **1997**, *8*, 1121−1125.

(17) Roche, P.; Al-Jowder, R.; Narayanaswamy, R.; Young, J.; Scully, P. *Anal. Bioanal. Chem.* **2006**, *386*, 1245−1257.

(18) Mills, A.; Lepre, A. *Anal. Chem.* **1997**, *69*, 4653−4659.

(19) Lee, S. K.; Okura, I. *Anal. Commun.* **1997**, *34*, 185−188.

(20) Koese, M. E.; Carrol, B. F.; Schanze, K. S. *Langmuir* **2005**, *21*, 9121−9129.

(21) Lamansky, S.; Djurovich, P.; Murphy, D.; Abdel-Razzaq, F.; Lee, H.; Adachi, C.; Burrows, P. E.; Forrest, S. R.; Thompson, M. E. *J. Am. Chem. Soc.* **2001**, *123*, 4304−4312.

(22) DeRosa, M. C.; Hodgson, D. J.; Enright, G. D.; Dawson, B.; Evans, C.; Crutchley, R. J. *J. Am. Chem. Soc.* **2004**, *126*, 7619−7626.

(23) Borisov, S. M.; Klimant, I. *Anal. Chem.* **2007**, *79*, 7501−7509.

(24) Vinogradov, S. A.; Lo, L. W.; Jenkins, W. T.; Evans, S. M.; Koch, C.; Wilson, D. F. *Biophys. J.* **1996**, *70*, 1609−1617.

(25) Kumar, R.; Ohulchanskyy, T. Y.; Roy, I.; Gupta, S. K.; Borek, C.; Thompson, M. E.; Prasad, P. N. *ACS Appl. Mater. Interfaces* **2009**, *1*, 1474−1481.

(26) Dunphy, I.; Vinogradov, S. A.; Wilson, D. F. *Anal. Biochem.* **2002**, *310*, 191−198.

(27) Khalil, G.; Gouterman, M.; Ching, S.; Costin, C.; Coyle, L.; Gouin, S.; Green, E.; Sadilek, M.; Wan, R.; Yearyean, J.; Zelelow, B. *J. Porphyrins Phthalocyanines* **2002**, *6*, 135−145.

(28) Papkovsky, D. B.; Ponomarev, G. V.; Trettnak, W.; O'Leary, P. *Anal. Chem.* **1995**, *67*, 4112−4117.

(29) Borisov, S. M.; Nuss, G.; Klimant, I. *Anal. Chem.* **2008**, *80*, 9435−9442.

(30) Aartsma, T. J.; Gouterman, M; Jochum, C.; Kwiram, A. L.; Pepich, B. V.; Williams, L. D. *J. Am. Chem. Soc.* **1982**, *104*, 6278−6283.

(31) Finikova, O. S.; Cheprakov, A. V.; Beletskaya, I. P.; Carroll, P. J.; Vinogradov, S. A. *J. Org. Chem.* **2004**, *69*, 522−535.

(32) Finikova, O. S.; Cheprakov, A. V.; Vinogradov, S. A. *J. Org. Chem.* **2005**, *70*, 9562−9572.

(33) Rogers, J. E.; Nguyen, K. A.; Hufnagle, D. C.; McLean, D. G.; Su, W.; Gossett, K. A.; Burke, A. R.; Vinogradov, S. A.; Pachter, R.; Fleitz, P. A. *J. Phys. Chem. A* **2003**, *107*, 11331−11339.

(34) Rozhkov, V. V.; Khajehpour, M.; Vinogradov, S. A. *Inorg. Chem.* **2003**, *2*, 4253−4255.

(35) Borisov, S. M.; Papkovsky, D. B.; Ponomarev, G. V.; DeToma, A. S.; Saf, R.; Klimant, I. *J. Photochem. Photobiol., A* **2009**, *206*, 87−92.

(36) Cheprakov, A. V.; Filatov, M. A. *J. Porphyrins Phthalocyanines* **2009**, *13*, 291−303.

(37) Kadish, K. M., Smith K. M., Guilard, R., Eds. *The Porphyrin Handbook*; Elsevier Science: New York, 2003; Vol. 15.

(38) Rosenow, T. C.; Walzer, K.; Leo, K. *J. Appl. Phys.* **2008**, *103*, 043105/1−043105/4.

(39) Borisov, S. M.; Nuss, G.; Haas, W.; Saf, R.; Schmuck, M.; Klimant, I. *J. Photochem. Photobiol., A* **2009**, *201*, 128−135.

(40) Galanin, N. E.; Kudrik, E. V.; Shaposhnikov, G. P. *Russ. J. Gen. Chem.* **2005**, *75*, 651−655.

(41) Borisov, S. M.; Klimant, I. *Dyes Pigm.* **2009**, *83*, 312−316.

(42) Bansal, A. K.; Holzer, W.; Penzkofer, A.; Tsuboi, T. *Chem. Phys.* **2006**, *330*, 118−129.

(43) Burczyk, A.; Loupy, A.; Bogdala, D.; Petit, A. *Tetrahedron* **2005**, *61*, 179−188.

(44) Neya, S.; Sato, T.; Hoshino, T. *Tetrahedron Lett.* **2008**, *49*, 1613−1615.

(45) Stuzhin, P. A.; Khelevina, O. G. *Coord. Chem. Rev.* **1996**, *147*, 41−86.

(46) Gouterman, M.; Wagniere, G. H.; Snyder, L. C. *J. Mol. Spectrosc.* **1963**, *11*, 108−127.

(47) Lebedev, A. Y.; Filatov, M. A.; Cheprakov, A. V.; Vinogradov, S. A. *J. Phys. Chem. A* **2008**, *112*, 7723−7733.

(48) Freyer, W.; Stiel, H.; Hild, M.; Teuchner, K.; Leupold, D. *Photochem. Photobiol.* **1997**, *66*, 596−604.

(49) Alford, P. C.; Cook, M. J.; Lewis, A. P.; McAuliffe, S. G.; Skarda, V.; Thomson, A. J. *J. Chem. Soc., Perkin Trans. II* **1985**, *5*, 705−709.

(50) Lai, S. W.; Hou, Y. J.; Che, C. M.; Pang, H. L.; Wong, K. Y.; Chang, C. K.; Zhu, N. *Inorg. Chem.* **2004**, *43*, 3724–3732.

(51) Vincett, P. S.; Voigt, E. M.; Rieckhoff, K. E. *J. Chem. Phys.* **1971**, *55*, 4131–4140.

(52) Carraway, E. R.; Demas, J. N.; DeGraff, B. A.; Bacon, J. R. *Anal. Chem.* **1991**, *63*, 337–342.

(53) Nagl, S.; Wolfbeis, O. S. *Analyst* **2007**, *132*, 507–511.

(54) Borisov, S. M.; Klimant, I. *Analyst* **2008**, *133*, 1302–1307.

(55) O'Donovan, C.; Hynes, J.; Yashunski, D.; Papkovsky, D. B. *J. Mater. Chem.* **2005**, *15*, 2946–2951.

(56) Borisov, S. M.; Mayr, T.; Klimant, I. *Anal. Chem.* **2008**, *80*, 573–582.

(57) Borisov, S. M.; Mayr, T.; Mistlberger, G.; Waich, K.; Koren, K.; Chojnacki, P.; Klimant, I. *Talanta* **2009**, *79*, 1322–1330.

(58) Finikova, O. S.; Lebedev, A. Y.; Aprelev, A.; Troxler, T.; Gao, F.; Garnacho, C.; Muro, S.; Hochstrasser, R. M.; Vinogradov, S. A. *Chem. Phys. Chem.* **2008**, *9*, 1673–1679.

(59) Estrada, A. D.; Ponticorvo, A.; Ford, T. N.; Dunn, A. K. *Opt. Lett.* **2008**, *33*, 1038–1040.

(60) Brias, R. P.; Troxler, T.; Hochstrasser, R. M.; Vinogradov, S. A. *J. Am. Chem. Soc.* **2005**, *127*, 11851–11862.

(61) Schubert, E. F. *Light Emitting Diodes*; Cambridge University Press: Cambridge, U.K., 2006; p 369.

(62) Perez, M. D.; Borek, C.; Forrest, S. R.; Thompson, M. E. *J. Am. Chem. Soc.* **2009**, *131*, 9281–9286.